Electronic Supplementary Material (ESI) for Nanoscale Horizons.

Supporting Information

Highly Stable Two-Dimensional Gold Selenide with Large In-Plane Anisotropy and Ultrahigh Carrier Mobility

*Cheng Tang[1], Lei Zhang[1], Chunmei Zhang[1], Jennifer MacLeod[1], Kostya (Ken) Ostrikov[1], and Aijun Du[1,]**

[1]School of Chemistry, Physics and Mechanical Engineering Queensland University of Technology, Gardens Point Campus, Brisbane, QLD 4001 (Australia)

* To whom correspondence should be addressed. Email: aijun.du@qut.edu.au (AD)

Optimized parameters

Table S1. Optimized parameters for bulk, monolayer, bilayer, and trilayer AuSe.

Parameters of AuSe	*a* (Å)	*b* (Å)	*c* (Å)	*β* (°)
Bulk	3.71	6.36	8.26	106.30
Bulk (exp.)[1]	3.66	6.26	8.35	106.03
Monolayer	3.65	5.97	-	-
Bilayer	3.67	6.15	-	-
Trilayer	3.68	6.19	-	-

Structures for bilayer and trilayer AuSe

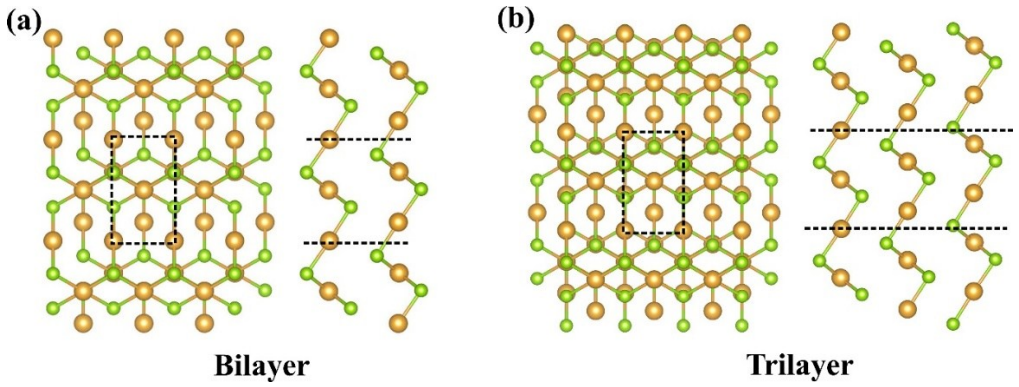

Figure S1. Top and side view of (a) bilayer and (b) trilayer AuSe nanosheets.

AIMD simulation for monolayer AuSe

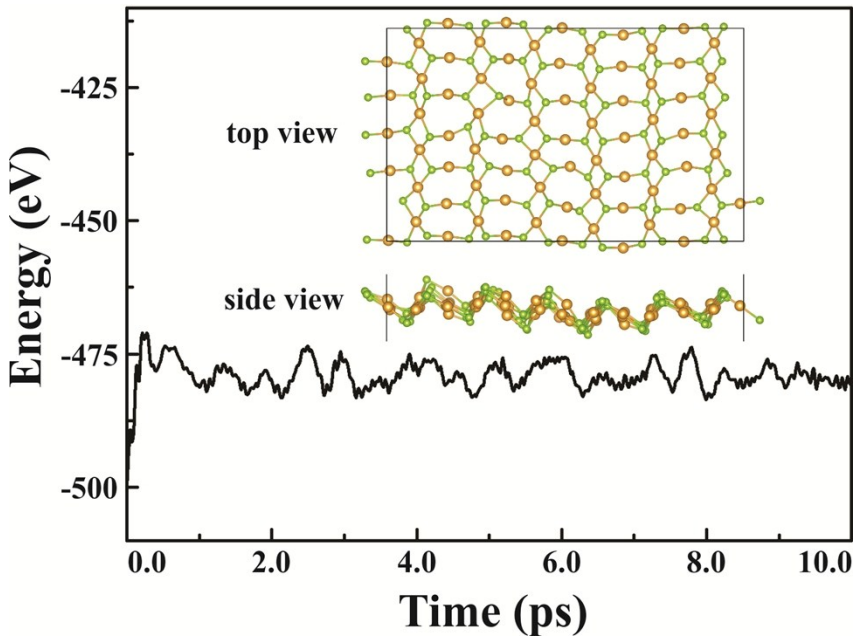

Figure S2. Total energy of monolayer AuSe under AIMD simulation at 1000 K. Top and side views of AuSe nanosheet at 10.0 ps are inserted.

Cleavage energies for bilayer and trilayer AuSe

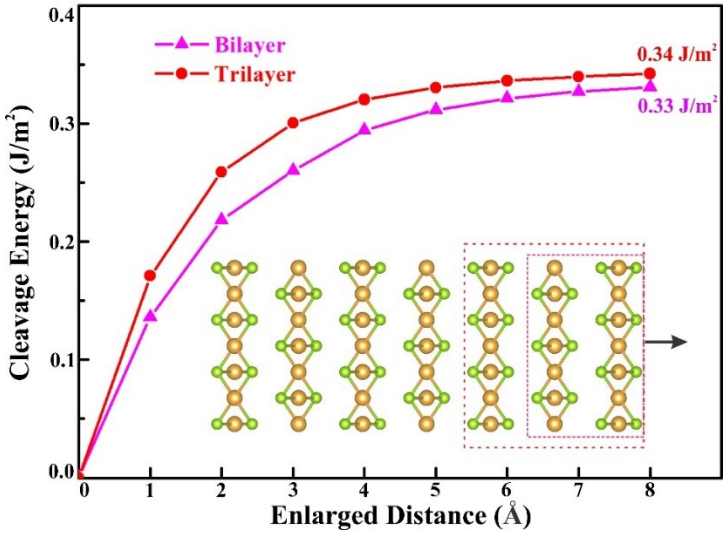

Figure S3. Cleavage energy of bilayer and trilayer AuSe as a functional of separation distance.

Density of states

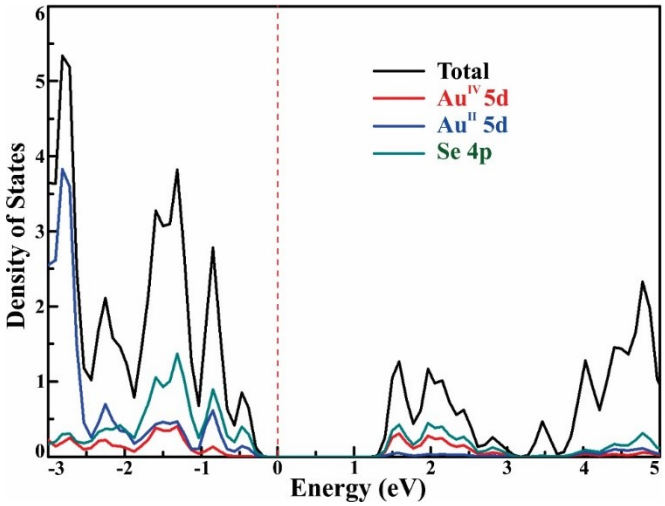

Figure S4. Density of states of monolayer AuSe.

Obital-resolved band structures

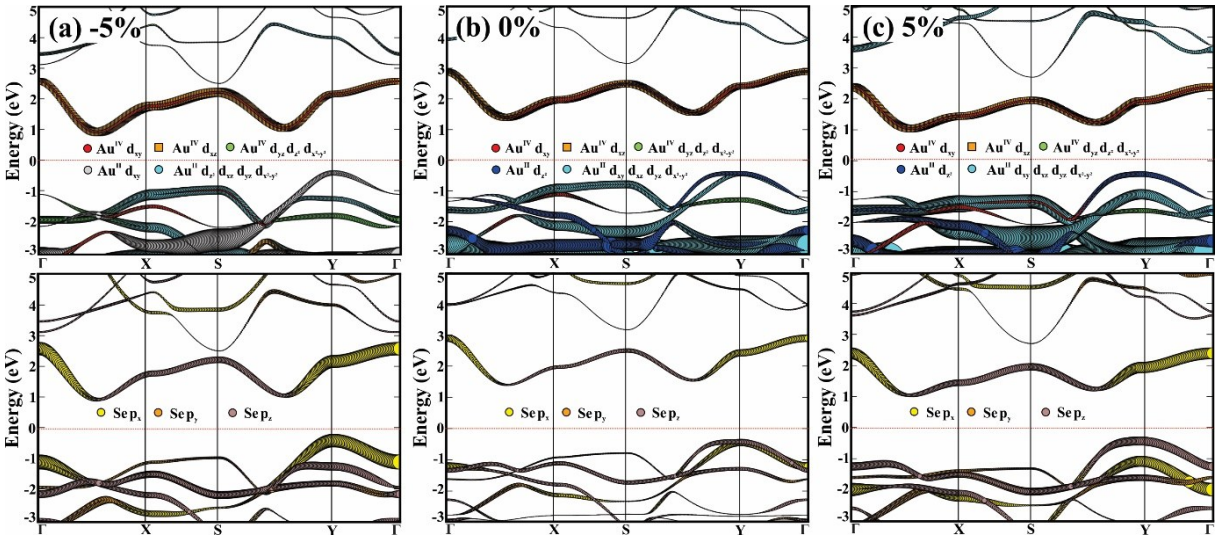

Figure S5. Orbital-resolved band structures of monolayer AuSe under ***a*** directional strains of (a) -5%, (b) 0% and (c) 5%, respectively.

Band structures for bilayer and trilayer AuSe

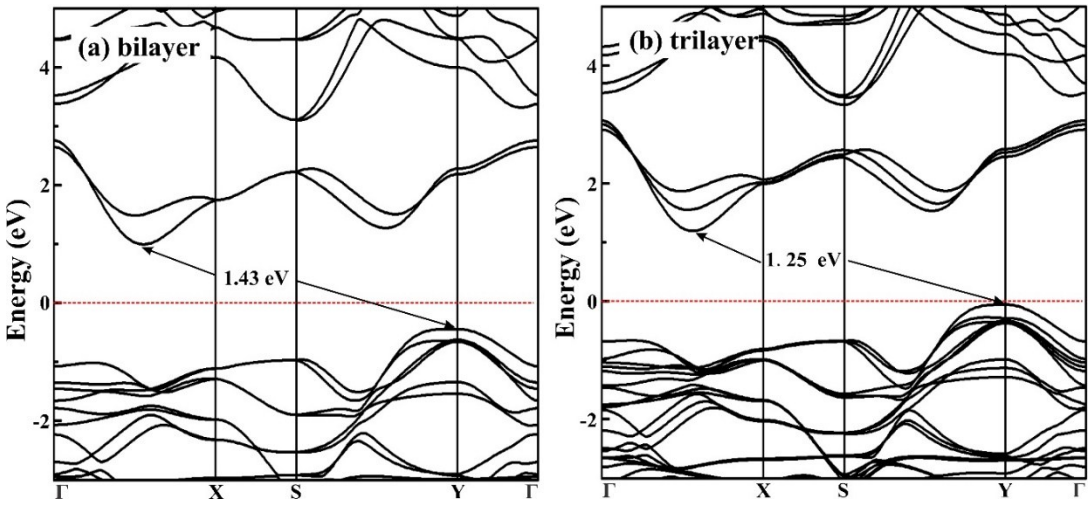

Figure S6. Band structures of bilayer and trilayer AuSe nanosheets.

Effects under uniaxial strain

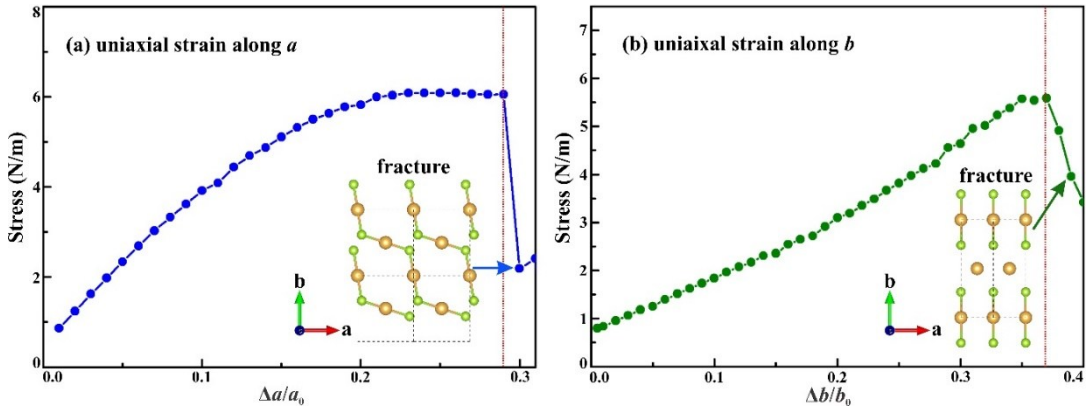

Figure S7. Stress in monolayer AuSe subjected to uniaxial strain along the (a) ***a*** and (b) ***b*** directions.

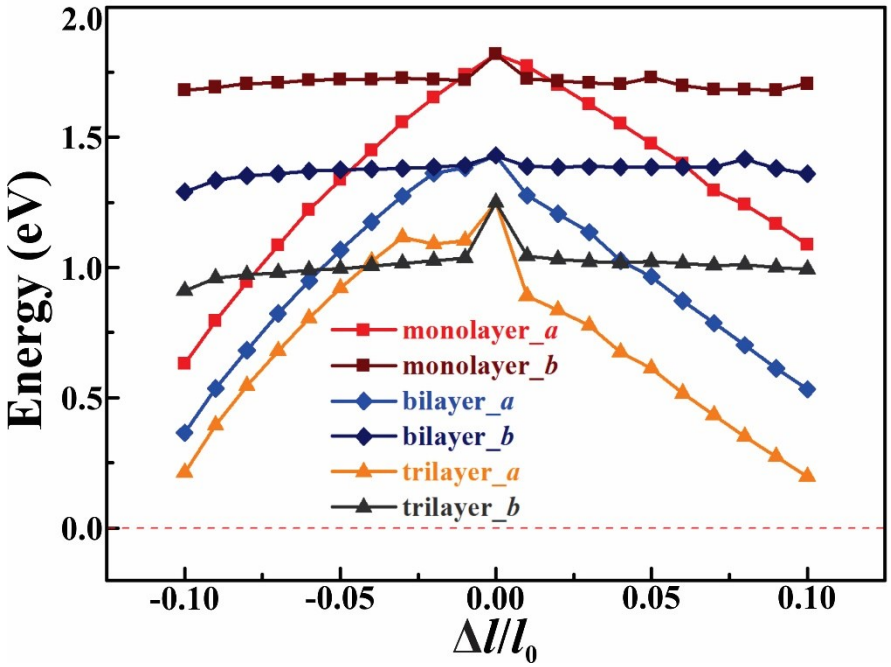

Figure S8. Band structures of monolayer, bilayer, and trilayer AuSe subjected to uniaxial strain from -10% to 10%.

Deformation potentials calculation

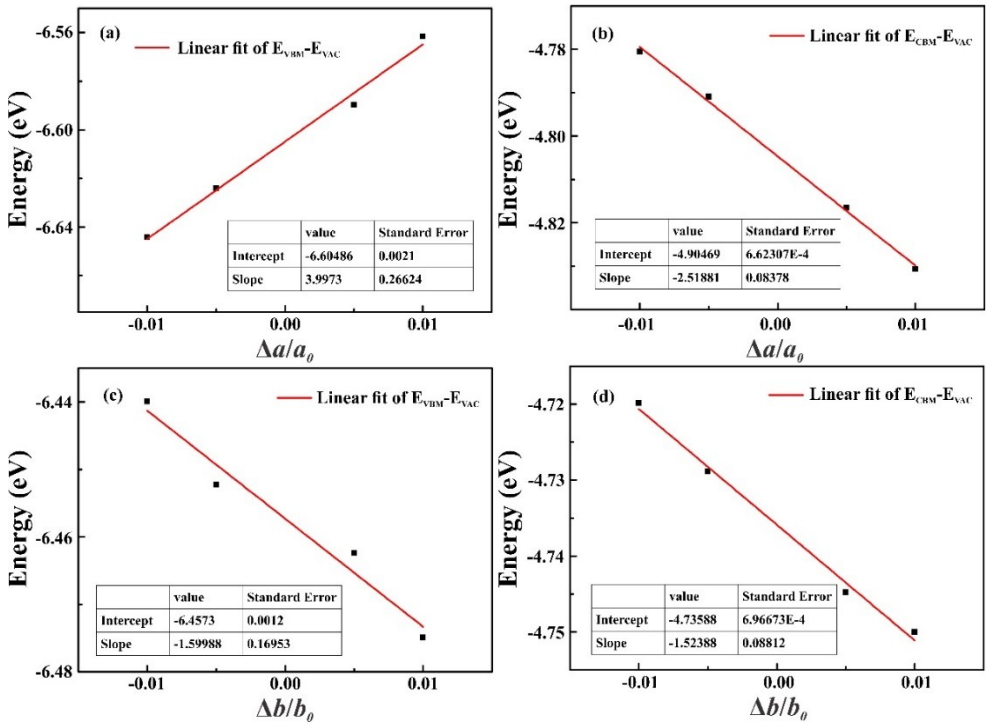

Figure S9. Linear fitting of deformation potential for monolayer AuSe along the (a, b) ***a*** direction and the (c, d) ***b*** direction. All the calculations are based on the HSE functional.

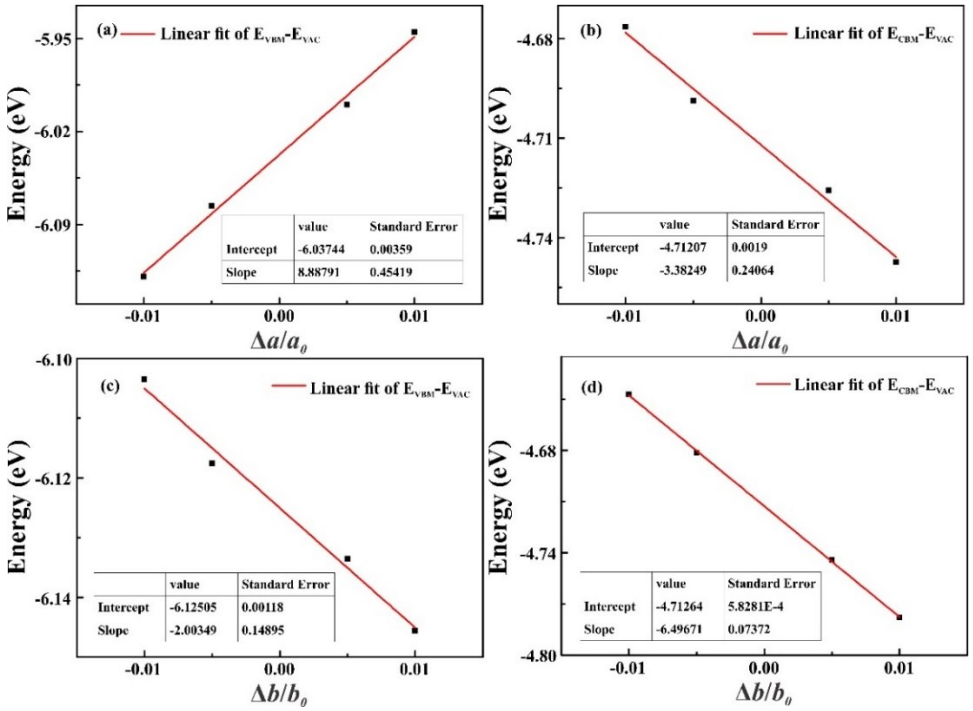

Figure S10. Linear fitting of deformation potential for bilayer AuSe along the (a, b) ***a*** direction and the (c, d) ***b*** direction.

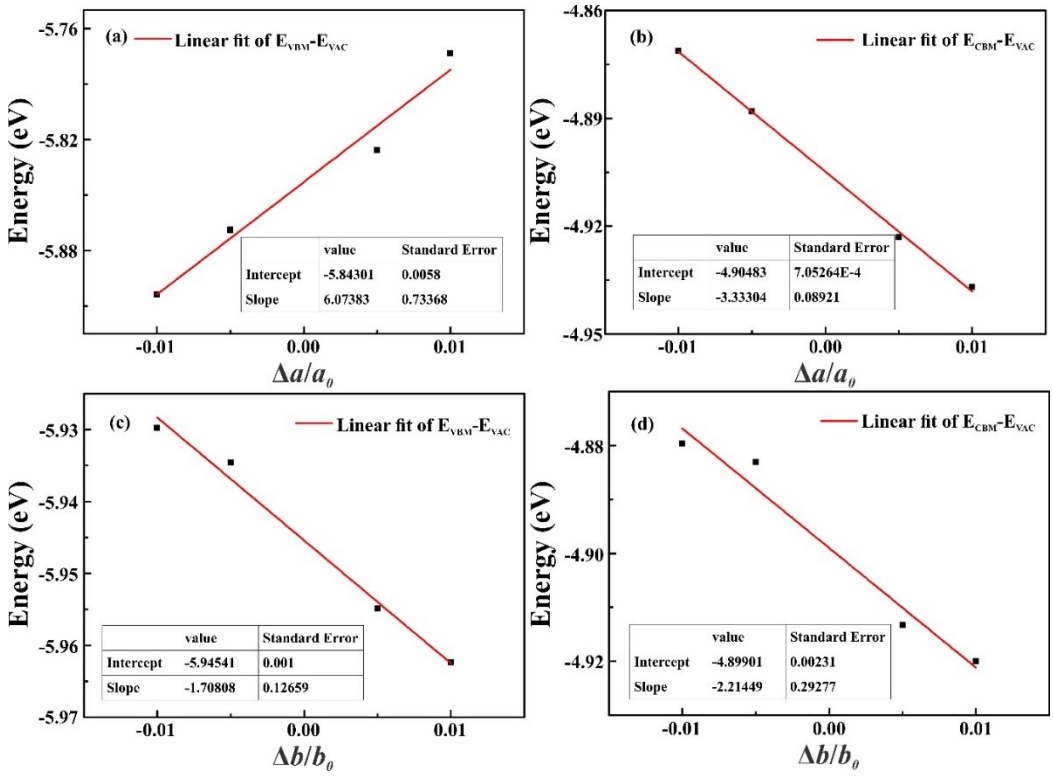

Figure S11. Linear fitting of deformation potential for trilayer AuSe along the (a, b) ***a*** direction and the (c, d) ***b*** direction.

Exciton effects

The exciton, a quasiparticle, is formed by the electrostatic Coulomb force between the photo-generated electron and hole. The exploration of excitonic effects in 2D AuSe is of high importance for evaluating potential applications in solar-energy conversion and light emission.[2] The excitonic effect of monolayer AuSe was studied by solving the *G0W0*-Bethe-Salpeter equation. Monolayer AuSe has an indirect bandgap of 2.28 eV (see Fig S12) using the *GW* method and the optical bandgap is calculated to be 1.97 eV. The direct *GW* bandgap of 2D AuSe (2.52 eV) is associated with the photo-excitation, thus the excitonic binding energy is estimated to be 0.55 eV, which is slightly smaller than that of 2H-MoS_2 (about 0.6 eV).[3] The excellent optical properties of 2D AuSe indicate considerable potential for optoelectronic applications.

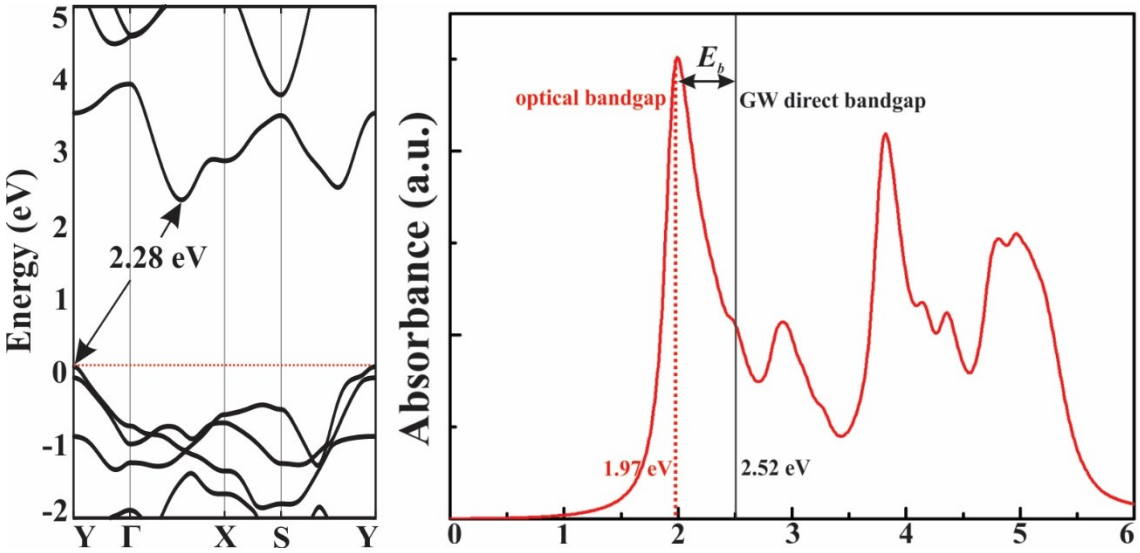

Figure S12. GW band structure of monolayer AuSe and BSE-optical absorption spectrum of monolayer AuSe. The Fermi level has been set to zero.

Spin orbital coupling (SOC)

To realize the effect of spin-orbital coupling (SOC) in the electronic calculations, we further compare the band structures for monolayer AuSe with and without SOC. As shown in Figure S13, AuSe remains indirect semiconductor with SOC effect, whereas the value of band gap is reduced to 1.58 eV. It is worth noting that no band splitting is introduced by the SOC effect at valance band maximum (VBM) and conduction band minimum (CBM) in AuSe. Then we examine the effect on the anisotropic carrier transport by calculating the effective mass along different directions. The CBM is still located along Γ-X direction, and the effective mass is 0.10 m_0, slightly smaller than the result without SOC. Besides, for VBM, it also locates at Y point and possesses strong anisotropic effective masses with the value of 0.59 and 0.10 m_0 along the ***a*** and ***b*** direction, respectively. Therefore, by considering the SOC effect, the 2D AuSe still keeps the anisotropically electronic properties. In addition, we further calculate the optical properties of monolayer AuSe. As shown in figure S13c, the absorption edge of AuSe shows the red-shift, due to the decreased band gap compared to the results without SOC effect. Thus, such effect gives AuSe a better performance on light absorption.

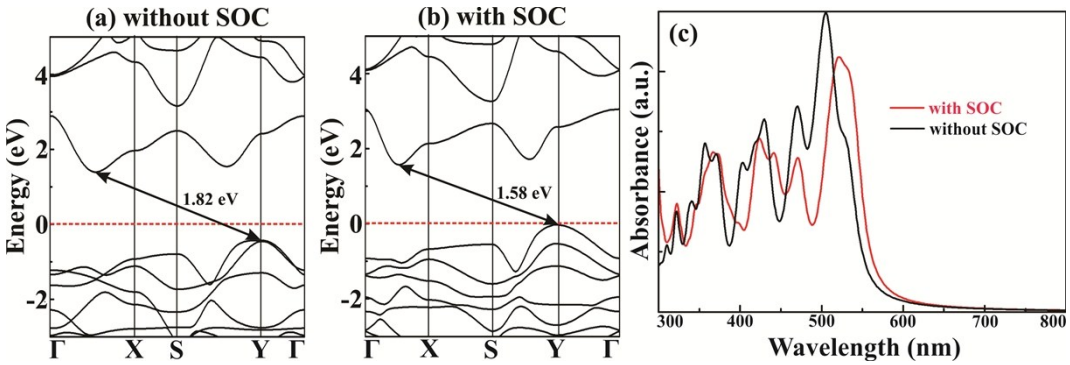

Figure S13. The band structures for monolayer AuSe (a) without and (b) with SOC effect. (c) Light absorption for monolayer AuSe.

Potential applications on Photocatalysis

In order to realize the potentials in photocatalytic, we calculated the energies of VBM/CBM of 2D AuSe, which can be obtained by:

$E_{VBM/CBM} = E_F - E_{Vac} + E_x$

where, E_{vac} and E_F represent the energy of the vacuum potential and Fermi level. E_x is the energy difference between VBM/CBM and the Fermi level. The electrostatic vacuum potentials (Figure S14) are 1.86 eV for monolayer, 3.02 eV for bilayer and 3.79 eV for trilayer AuSe, respectively. Therefore, the positions of VBM and CBM are illustrated in the schematic Figure S15. As a comparison, we plot the potentials of three common reaction, including oxygen oxidation, hydrogen reduction and CO_2 reduction. Herein, the band positions of 2D AuSe is suitable for diving the oxygen oxidation reaction, but unavailable for other two reactions. However, the band edges can be effectively adjusted by fabricating AuSe with other suitable semiconductors, suggesting an improved performance on photocatalysis. It is worth mentioning that photocatalytic performance is also limited by other factors rather than the suitable band edges and excellent light absorption. This is deserved to be studied in the future theoretical and experimental works.

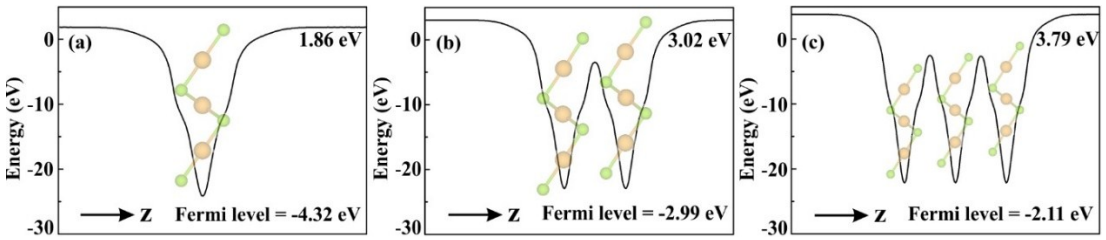

Figure S14. Electrostatic vacuum potential of (a) monolayer, (b) bilayer and (c) trilayer AuSe. The fermi energies are listed in the figure.

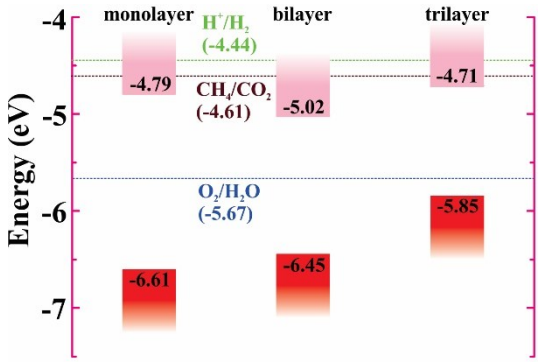

Figure S15. The schematic diagram of band edges of 2D AuSe.

Reference

1. Rabenau, A.; Schulz, H. *Journal of the Less Common Metals* **1976,** 48, (1), 89-101.
2. Pospischil, A.; Furchi, M. M.; Mueller, T. *Nature nanotechnology* **2014,** 9, (4), 257.
3. Jiang, Z.; Liu, Z.; Li, Y.; Duan, W. *Phys. Rev. Lett.* **2017,** 118, (26), 266401.